ISSN 1068-3356, Bulletin of the Lebedev Physics Institute, 2018, Vol. 45, No. 1, pp. 1–5. © Allerton Press, Inc., 2018.
Original Russian Text © N.A. Dyuzhev, G.D. Demin, T.A. Gryazneva, A.E. Pestov, N.N. Salashchenko, N.I. Chkhalo, F.A. Pudonin, 2018, published in Kratkie Soobshcheniya po Fizike, 2017, Vol. 44, No. 12, pp. 56–63.

Microfocus X-Ray Tubes with a Silicon Autoemission Nanocathode as an X-Ray Source

N. A. Dyuzhev[a], G. D. Demin[a], T. A. Gryazneva[a], A. E. Pestov[b], N. N. Salashchenko[b], N. I. Chkhalo[b], and F. A. Pudonin[c]

[a] *National Research University of Electronic Technology (MIET), pl. Shokina 1, Zelenograd, Moscow oblast, 124498 Russia; e-mail: gddemin@gmail.com*
[b] *Institute for Physics of Microstructures, Russian Academy of Sciences, ul. Ul'yanova 46, Nizhni Novgorod, 603950 Russia*
[c] *Lebedev Physical Institute, Russian Academy of Sciences, Leninskii pr. 53, Moscow, 119991 Russia*

Received December 8, 2017

Abstract—To develop nanostructures with extremely low spatial resolution (to 10 nm and below), a new concept of the use of arrays of microfocus X-ray tubes based on field emission silicon nanocathodes is proposed. A new λ-tunable microfocus source of X-ray radiation, based on a thin-film transmission target with field emission nanocathode with tunable wavelength, is proposed. The possibility of decreasing the exposed area size to 20 nm and smaller by varying the tube blocking voltage is shown. The use of these X-ray sources opens a new way of developing maskless X-ray lithography.

DOI: 10.3103/S1068335618010013

Keywords: field emission cathode, maskless X-ray lithography, microfocus X-ray tube, field emission, nanostructures, vacuum nanoelectronics.

Currently, extensive studies directed to the search for the methods for developing transistor structures with topological sizes to 1–3 nm are in progress [1], which is necessary to develop various devices of nano- and optoelectronics, microelectromechanical systems (MEMS), and others. The key technology in modern semiconductor electronics is projection photolithography. The nanoscale resolution is achieved due to the use of various image enhancement methods [2]. Currently, to 70% of nanoelectronic devices are produced using this technology. Almost a tenfold excess of the diffraction limit of the effective wavelength of the lithograph (193 nm) results in an increase in the process and equipment cost, and, as the experience shows, image enhancement methods almost ran their course. The solution to this problem seems to be the use of projection photolithography in extreme ultraviolet (EUV lithography) with an effective wavelength of 13.5 nm in forming the critical-size spot on the chip [3]. However, this technology is also associated with a number of problems which do not allow advance to the sub-10-nanometer lithography region [4], which are, e.g., insufficient productivity for mass production, EUV source service life, difficult achievement of numerical aperture of projection objective $NA > 0.5$, and others. Due to the EUV mask features (reflective multilayer structure a few hundreds of nanometers thick, coated with an absorbing ($\sim$100 nm) layer), due to the shadowing effects, absolutely nonstandard schemes are required, in particular, the use of an objective with different demagnification in perpendicular directions [5]. At present, the most promising direction is multibeam electron lithography, where certain progress is already achieved. However, here are also serious problems associated with wafer heating, interaction of electron beams, and a high cost of such a lithograph ($\sim$100 millions of euro).

One of the possible solutions of the above problems is maskless X-ray nanolithography (MXNL) proposed for the first time in [6]. Interest in this technology arose after the studies [7, 8] where it was shown for the first time that this technology has a potentially high resolution to 20 nm and productivity comparable to conventional projection lithography. In such an X-ray lithograph, dynamically controlled MEMS micromirrors play the role of the virtual mask, and a laser–plasma source is used as an X-ray source.

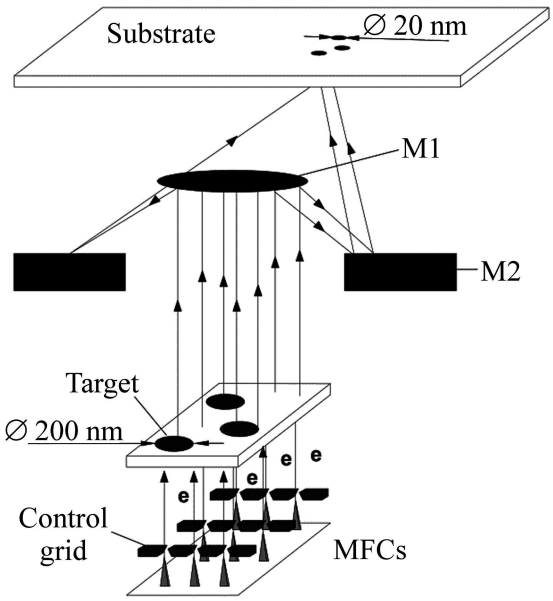

Fig. 1. Schematic diagram of the X-ray nanolithograph based on the array of microfocus X-ray tubes from field emission nanocathodes (MFCs) with the X-ray optical radiation focusing system, where M1, M2 is the system of multilayer interference mirrors.

In the present study, as an alternative to the laser–plasma X-ray source and MEMS, we propose the use of microfocus X-ray tube arrays. A distinctive feature of the proposed concept is the use of triode systems of field emission nanocathodes with a control electrode grid as microfocus tubes and a transmission target representing an X-ray transparent membrane with a thin metal film. The field emission nanocathode represents a silicon tip with nanoscale emitting surface, which generates an emission current sufficient to cause X-ray emission in the target as a voltage above the blocking voltage is applied to grid electrodes. This is shown in Fig. 1 demonstrating the general schematic of the nanolithograph with field emission nanocathode array.

The choice of beryllium as a target material makes it possible to obtain X-ray radiation at a wavelength of 11.4 nm, which can be efficiently focused using a system of multilayer interference Mo(Ru)/Be mirrors with a reflectance higher than 70%, which significantly simplifies the nanolithograph scheme and opens the way to a decrease in lithographic sizes to 20 nm and smaller [8]. Table 1 lists some parameters of microfocus X-ray tubes based on field emission nanocathodes.

The basis of an individual microfocus X-ray tube is a cathode unit consisting of a field emission cathode and a control grid electrode, and an anode electrode with a transmission target (see Fig. 2(a)). At certain anode and grid potentials, an electric field is formed on the cathode surface, which is sufficient for field emission of hot electrons, which results in the formation of the electron beam incident on a metal target and specifying the generation area of output X-ray radiation (Fig. 2(b)).

Thus, using fine focusing of the electron beam, it is intended to create directed X-ray radiation using a mirror system and to perform operations of maskless X-ray lithography with an ultimate resolution to 10 nm, which becomes possible using X-ray optics [9]. Figure 3 shows the results of simulation of the electronic system of the microfocus X-ray tube, which demonstrate the possibility of varying the electron beam size by varying the negative blocking voltage at the grid electrode, which makes it possible to decrease the electron spot diameter D_B on the transmission target to 200 nm and smaller. The cathode tip radius and the hole diameter in the grid electrode were set to 5 nm and 400 nm, respectively. Figure 3 shows that a lower blocking voltage V_G is required to reduce the tube spot as the cathode–anode distance D_{CA} increases in the given range from 400 nm to 600 nm.

We previously proposed the model of the X-ray source with field emission nanocathode and determined optimum parameters allowing the maximum intensity of X-ray radiation emerging from the target and the high resolution [10]. On its basis, the concept of the microfocus X-ray source with tunable spectrum was proposed. This source consists of a thin-film transmission target with field

Table 1. Parameters of X-ray tubes based on field emission nanocathodes

Parameters of the X-ray emitter based on a field emission nanocathode array	
Electron beam spot diameter	200 nm
X-ray source size	10 mm × 10 mm ($2.5 \cdot 10^7$ pixels)
Parameters of the X-ray nanolithograph with an emitter based on a field emission nanocathode array	
X-ray wavelengths	11.4 nm
Objective NA	0.5
Input NA	0.05
Demagnification	10×
Pixel size on the wafer with photoresist	20 nm
Reflectance of multilayer interference structures (MIS)	70%
Exposure dose for a sensitive resist	10 mJ/cm^2

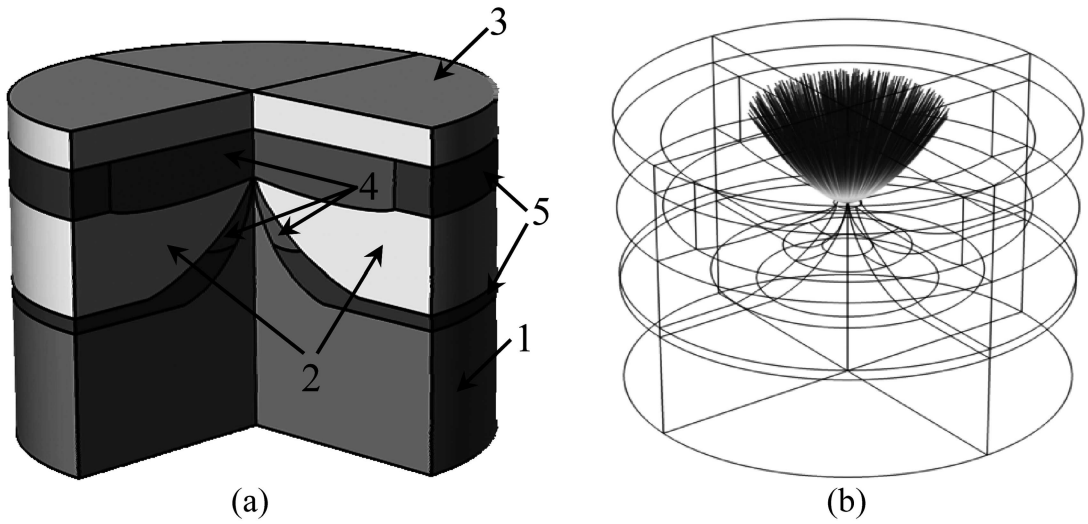

Fig. 2. (a) Proposed design of the single X-ray tube: (1) field emission cathode, (2) grid electrode, (3) anode with transmission target, (4) vacuum gap, (5) dielectric spacers; (b) Image of the electron beam emitted from the cathode surface (the electron trajectory is shown at positive anode voltage V_A and grid voltage $V_G = 0$ V).

emission cathode with tunable wavelength. The tuning is implemented by striking the targets of given composition and material with electron beam, which provides a required spectrum of characteristic radiation. Such an approach with wavelength tuning affects the directivity and angular resolution of the most part of generated radiation for different types of its polarization, which makes it possible to vary the angular radiation directivity and can be applied to the formation of nanoscale topological elements of layers of functional electronics [11]. Thus, Fig. 4 shows the results of calculations of the spatial distribution of the X-ray radiation generated in the thin metal film of the transmission target consisting of different materials (Be, Ta, W). The target material was chosen taking into account the single peak of the characteristic wavelength in the case of the anode voltage V_A varied from 500 to 2500 V. We can see that the spatial distribution is uniform over the angle for σ-polarization of radiation; in the case of

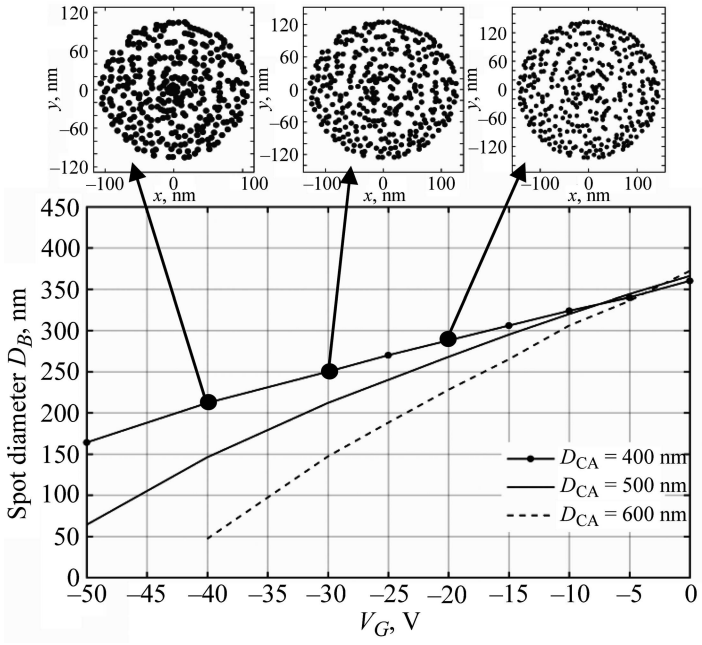

Fig. 3. Dependence of the spot diameter D_B on the target on the blocking voltage V_G at the grid electrode (at the anode voltage $V_A = 500$ V) for various cathode–anode distances D_{CA} in the electronic system of the microfocus X-ray tube under study.

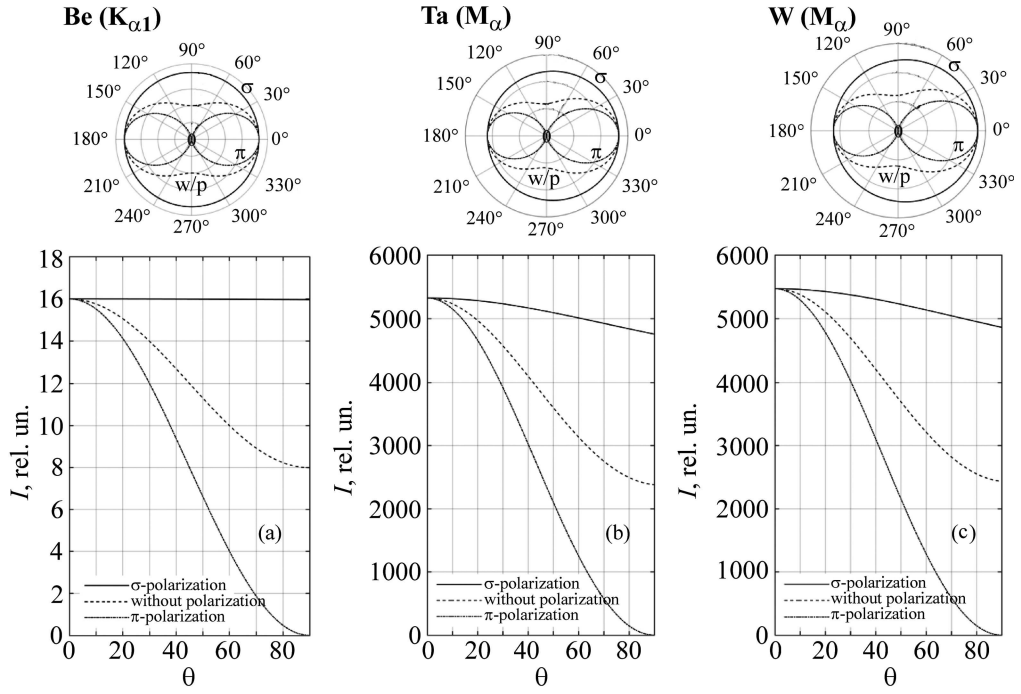

Fig. 4. Spatial (angular) distribution of the intensity I of X-ray radiation of different polarizations (σ-polarization, unpolarized radiation, π-polarization) generated in targets of different compositions (Be ($K_{\alpha 1}$), Ta (M_α), W (M_α)) at the anode voltage $V_A = 2500$ V. The curves are normalized to the maximum.

π-polarization, radiation takes pronounced directivity. In turn, the angular distribution of unpolarized radiation is intermediate between radiation with σ- and π-polarization. For wavelengths of $K_{\alpha 1}$ (Be) and M_α (Ta, W) characteristic radiation generated in the tube, the behavior of the dependences of the intensity I on the solid angle θ slightly differ from each other, which can be seen in the figures.

Table 2. Solid angle θ' within which 80% of X-ray radiation generated in the target (Be, Ta, W) are concentrated at the anode voltage $V_A = 2500$ V

Target material	Be ($Z = 4$)			Ta ($Z = 73$)			W ($Z = 74$)		
Radiation polarization	σ	π	unpolarized.	σ	π	unpolarized.	σ	π	unpolarized.
θ', deg.	71.98	43.38	64.57	71.01	42.81	63.34	70.97	42.79	63.29

Table 2 generalizes the conclusions on the obtained dependences of the radiation intensity on its angular directivity, where the angle θ' is calculated which encloses 80% of the total X-ray flux generated in the transmission target. Taking into account radiation polarization type variation, it was found that the angular directivity varies in the range from 43° to 72°. This makes it possible to control the exposure region size during maskless X-ray lithography. In view of the simplicity of the scheme of the proposed X-ray nanolithograph with such an X-ray source, the absence of an expensive and large laser-plasma source of soft X-ray radiation and MEMS, an inexpensive nanolithography can be developed, which has no world analogs.

Thus, a new concept of the nanolithograph based on the microfocus X-ray tube array as an X-ray source was proposed. It was shown that lithographic sizes can be reduced in this case to 20 nm and smaller. This allowed us to propose a new microfocus X-ray source with tunable spectrum, based on a thin-film transmission target with field emission nanocathode with tunable wavelength. In our opinion, the proposed concept of the microfocus X-ray source can become a basis for developing new technologies in the field of nanolithography and will solve a number of key scientific and technological problems in micro- and nanoelectronics.

ACKNOWLEDGMENTS

This study was performed on the equipment of the Collective use center “MST and EKB” and supported by the Ministry of Education and Science of the Russian Federation, contract no. 14.578.21.0188 (RFMEFI57816X0188).

REFERENCES

1. M. M. Waldrop, Nature **530**, 7589 (2016).
2. https:// 4pda.ru/2017/03/29/338955.
3. B. Wu and A. Kumar, Appl. Phys. Rev. **1**, 011104 (2014).
4. http://semimd.com/blog/2016/11/28/high-na-euv-lithography-investment/.
5. I. Servin et al., Proc. SPIE **9423**, 94231C (2015).
6. N. Choksi et al., J. Vac. Sci. Technol. B **17**, 3047 (1999).
7. N. I. Chkhalo, V. N. Polkovnikov, N. N. Salashchenko, and M. N. Toropov, Proc. SPIE **10224**, 1022410-1-08 (2016).
8. N. I. Chkhalo and N. N. Salashchenko, AIP Advances **3**, 082130 (2013).
9. J. Zhao, Y. Wu, C. Xue, et al., Microelectron. Eng. **170**, 49 (2017).
10. N. A. Dyuzhev et al., Poverkhnost No. 4, 1 (2017) [J. Surf. Invest.: X-ray, Synchrotron Neutron Tech. **11**, 443 (2017)].
11. V. A. Bespalov et al., Poverkhnost [J. Surf. Invest.: X-ray, Synchrotron Neutron Tech.] (in press).